

Advanced technology of thermal decomposition for AMBN and ABVN by DSC and VSP2

Shang-Hao Liu · Chi-Min Shu

Received: 4 October 2014 / Accepted: 10 February 2015 / Published online: 29 March 2015
© Akadémiai Kiadó, Budapest, Hungary 2015

Abstract In addition to organic peroxides, azo compounds are important basic initiators applied in chemical plants. In general, these compounds decompose at lower temperatures than aldehydes, ketones, and ethers, some of which decompose unimolecularly at higher temperatures so that the first products are not as stable due to the bivalent $-N=N-$ composition, which has very active characteristics. In this study, thermal stability tests of two azo compounds, 2,2'-azobis (2-methylbutyronitrile) and 2,2'-azobis-(2-4-dimethylvaleronitrile), were evaluated via differential scanning calorimetry to determine the apparent exothermic onset temperature (T_0), heat of decomposition (ΔH_d), and apparent exothermic peak temperature (T_p) for intrinsic thermal safety analysis. Following the dynamic tests, vent sizing package 2 (VSP2) was employed to determine the maximum pressure (P_{max}), maximum temperature (T_{max}), maximum self-heating rate $[(dT/dt)_{max}]$, maximum pressure rise rate $[(dP/dt)_{max}]$, and adiabatic time to maximum rate $[(TMR)_{ad}]$ under a credible case. Finally, we attempted to obtain the apparent activation energy (E_a) and pre-exponential factor (A) during decomposition via a non-isothermal approach through Flynn–Wall–Ozawa equation and the approximate solution for the design of safer reaction conditions

with greater efficiency when azo compounds are used as initiators. As a whole, a prudent approach for the integration of thermal hazard data was developed that is necessary and useful for determining a proactive emergency response procedure associated with industrial applications on azo compounds during thermal upsets.

Keywords Approximate solution · Azo compounds · Differential scanning calorimetry (DSC) · Flynn–Wall–Ozawa equation · Vent sizing package 2 (VSP2)

List of symbols

A	Pre-exponential factor (min^{-1})
C_a	Concentration of the sample (M)
C_{a0}	Initial concentration of the sample (M)
E_a	Apparent activation energy (kJ mol^{-1})
ΔH_d	Heat of decomposition (J g^{-1})
P	Pressure (bar)
P_{max}	Maximum pressure (bar)
$(dP/dt)_{max}$	Maximum pressure rise rate (bar min^{-1})
t	Time (min)
T	Temperature ($^{\circ}\text{C}$)
T_0	Apparent exothermic onset temperature ($^{\circ}\text{C}$)
T_{max}	Maximum temperature ($^{\circ}\text{C}$)
T_p	Peak temperature ($^{\circ}\text{C}$)
$(dT/dt)_{max}$	Maximum temperature rise rate ($^{\circ}\text{C min}^{-1}$)
α	Degree of conversion of a component (dimensionless)
β	Scanning rate ($^{\circ}\text{C min}^{-1}$)

S.-H. Liu
Department of Safety, Health, and Environmental Engineering,
National Yunlin University of Science and Technology
(YunTech), 123, University Rd., Sec. 3, Douliou, Yunlin 64002,
Taiwan, ROC

C.-M. Shu (✉)
Process Safety and Disaster Prevention Laboratory, Department
of Safety, Health, and Environmental Engineering, YunTech,
123, University Rd., Sec. 3, Douliou, Yunlin 64002, Taiwan,
ROC
e-mail: shucm@yuntech.edu.tw

Introduction

Azo compounds are classified as Class IV in the UN classification because of the potential risk of decomposition

from self-heating during storage and transportation [1, 2]. The compounds include the bivalent $-N=N-$ composition, which may be easily cleaved and release large amounts of heat and gas under a high temperature or other hazardous scenarios [3, 4]. The breaking of the bivalent bond composition leads to a rapid increase in temperature and pressure, which triggers a runaway reaction that leads to a fire or explosion while the cooling system fails or another upset scenario emerges [5–7].

Liu et al. [2] initially observed the incompatible reaction of 2,2'-azobis (isobutyronitrile) (AIBN) and obtained the exothermic behaviours, AIBN mixed with acid or alkaline material, via differential scanning calorimetry (DSC) and thermal activity monitor III. To emphasize the safe concerns, the purpose of our study was further to focus on the thermal behaviours of two typical self-reactive azo compounds, 2,2'-azobis (2-methylbutyronitrile) (AMBN) and 2,2'-azobis-(2-4-dimethylvaleronitrile) (ABVN) for inherent safety properties via hybrid methods [1, 3, 4]. The structure of two azo compounds is depicted in Fig. 1. Upon decomposition, AMBN and ABVN can release nitrogen and other toxicities, isobutyronitrile and acrylonitrile, to the environment, which could cause injuries because many nitrile compounds evolve during meltdown and undergo rapid decomposition from 100 to 107 °C [1, 8, 9]. In addition, fire or explosion may also occur. Because AMBN

and ABVN will slowly decompose at room temperature [8, 9], they should be stored at temperatures below 10 °C and removed from fire and any prominent external thermal sources.

In the current study, we determined the thermal stability parameters of AMBN and ABVN to investigate the corresponding thermal hazard under non-isothermal and adiabatic conditions. Thermal stability tests were conducted using DSC to acquire thermokinetic parameters, including apparent exothermic onset temperature (T_0), exothermic peak temperature (T_p), and heat of decomposition (ΔH_d). The runaway reaction under adiabatic conditions was, in turn, mimicked by using vent sizing package 2 (VSP2) to determine the temperature (T) and pressure (P) with respect to time (t) during the process, as well as the thermal stability data in the thermal runaway reaction, including maximum pressure (P_{max}), maximum temperature (T_{max}), maximum self-heating rate $[(dT/dt)_{max}]$, and maximum pressure rise $[(dP/dt)_{max}]$. As a whole, the advanced experimental method from small scale (mg) of DSC and large scale (g) of VSP2 was adopted to evaluate the thermal stability parameters to design safer process conditions, appraise all types of related thermal risks, and establish the risk assessment techniques of the new process [10–14].

Experimental and methods

Dynamic test

The experimental analysis was performed using Mettler DSC821^e and the analysis software STAR^e [15, 16]. DSC was used for the preliminary thermal analysis of the substance to acquire data for the exothermic curve, released heat, and thermal behaviours. In the DSC test, AMBN and ABVN were imbedded in a gold crucible. The heating rates were set at 0.5, 1, 2, 4, and 8 °C min⁻¹, and the heating range was between 30 and 300 °C.

Adiabatic test

VSP2, produced by Fauske & Associates, LLC [17, 18], was applied to measure the adiabatic state which can simulate the reactor in the process. Then the heat-wait-search mode can provide the dynamic scanning test from room temperature to apparent exothermic onset temperature to obtain temperature and pressure trace versus time in the test cell (ca. 112 mL) [17, 18]. The thermokinetic and pressure behaviours in the same test cell can typically be tested without issues in its extrapolation to the commercial scale because of the low thermal inertia factor (Φ) of approximately 1.05–1.32.

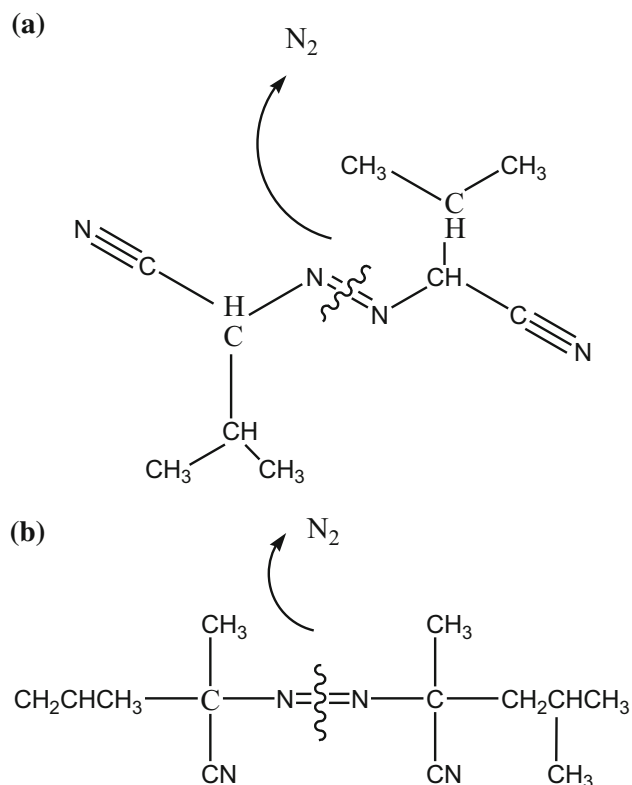


Fig. 1 Structure of two azo compounds. **a** AMBN, **b** ABVN [1, 2, 4]

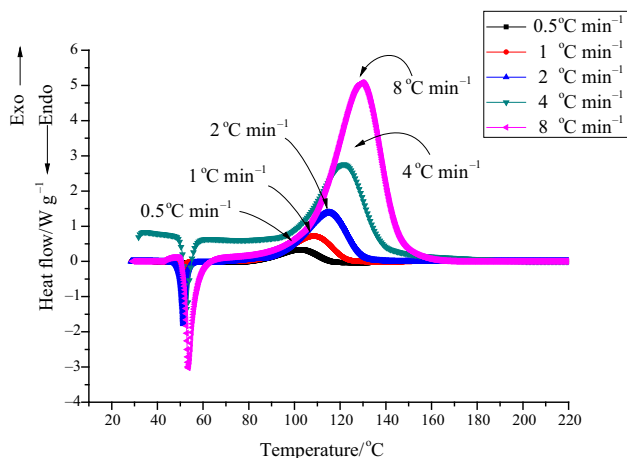


Fig. 2 DSC thermal curves of heat flow versus temperature for AMBN by DSC with β of 0.5, 1, 2, 4, and 8 °C min⁻¹

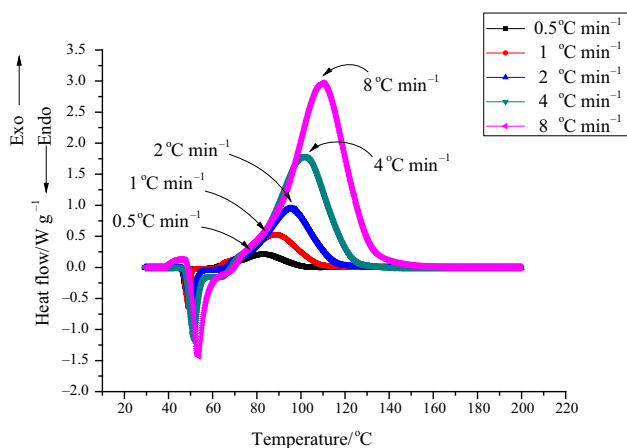


Fig. 3 DSC thermal curves of heat flow versus temperature for ABVN by DSC by DSC with β of 0.5, 1, 2, 4, and 8 °C min⁻¹

Results and discussion

DSC test results

The mass concentration of 98 mass% for AMBN and ABVN was measured using the DSC821^c with a differential scanning analysis function, which was used to determine the preliminary thermal stability and the exothermic phenomenon of the thermal decomposition reaction. To estimate the chemical kinetic parameters of the AMBN and ABVN, we measured the thermal power profiles in a dynamic mode. As shown in Figs. 2, 3, different scanning rates of AMBN and ABVN between 0.5 and 8 °C min⁻¹ generated a different exothermic reaction after heating, with a heating range between 30 and 300 °C.

According to the exothermic peak temperatures listed in Table 1, T_0 of AMBN and ABVN was approximately 81

Table 1 Experimental results for AMBN and ABVN via DSC test at 0.5, 1, 2, 4, and 8 °C min⁻¹

$\beta/^\circ\text{C min}^{-1}$	Mass/mg	$T_m/^\circ\text{C}$	$T_0/^\circ\text{C}$	$T_p/^\circ\text{C}$	$\Delta H_d/\text{J g}^{-1}$
AMBN					
0.5	5 ± 0.2	50	81	102	859
1.0		51	88	108	902
2.0		51	94	115	955
4.0		54	101	121	781
8.0		56	107	130	952
ABVN					
0.5		49	61	83	555
1.0		49	64	88	764
2.0		51	63	95	765
4.0		52	67	101	786
8.0		54	75	109	574

and 61 °C, respectively, ΔH_d was approximately 859 and 555 J g⁻¹, and T_p was approximately 102 and 83 °C at 0.5 °C min⁻¹. The average heat of reaction of the AMBN and ABVN was 889 and 689 J g⁻¹, respectively, and was therefore classified as highly hazardous substances because the exothermic reaction heats were >250 J g⁻¹.

On the other hand, the researchers discovered, by using DSC or accelerating rate calorimeter (ARC), that the endothermic melting peak overlapped the exothermic decomposition peak, resulting in the uncertainty of the initial decomposition temperature for azo compounds in the past studies [1–8]. In Figs. 2, 3, when the solid melted, a thermal decomposition reaction followed in accordance with the continuous parallel equation and heat scanning of the solid sample occurred while the material was not clearly separated yet [1–8]. Overall, after the catalytic decomposition of AMBN and ABVN, a tremendous amount of heat was generated.

Computation of thermokinetic parameters using the Flynn–Wall–Ozawa equation

This method is applicable to the DSC integral-type thermal curves. Flynn and Wall [19] and Ozawa [20] proposed the isoconversional method, Flynn–Wall–Ozawa equation, using TG/DSC curves to determine kinetic parameters of reactions. The following equation can be represented on the basis of the Doyle approximation [21] for heterogeneous chemical reactions:

$$\log(\beta) = \log\left(\frac{AE_a}{R}\right) - \log[g(\alpha(T))] - 2.315 - 0.4567 \frac{E_a}{RT} \quad (1)$$

In Eq. (1), $g(\alpha(T))$ is a conversional function, E_a is the apparent activation energy, R is the gas constant, and A is a

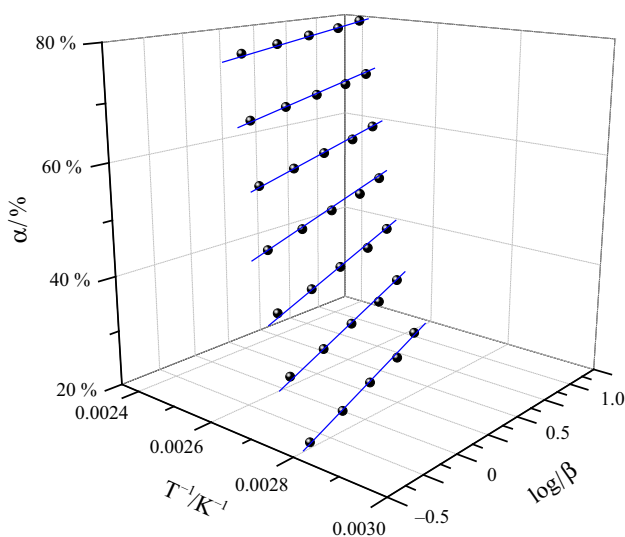


Fig. 4 Activation energy analysis graphs for AMBN at scanning rates of 0.5, 1, 2, 4, and 8 °C min⁻¹ under α at 20, 30, 40, 50, 60, 70, and 80 by Ozawa–Flynn–Wall kinetic equation

pre-exponential factor. The principle of isoconversional method is based on the assumption that the reaction rate at a given degree of conversion is only a function of the temperature. Therefore, for different heating rates at a constant degree of conversion $g(\alpha(T))$, a linear relationship is observed by plotting $\log(\beta)$ versus T^{-1} and E_a is obtained as the slope of the straight line.

The apparent activation energy analysis graphs for AMBN and ABVN at scanning rates of 0.5, 1, 2, 4, and 8 °C min⁻¹ using the kinetic equation are delineated in Figs. 4, 5. From Table 2, the E_a values, computed from the kinetic equation, are 143 and 128 kJ mol⁻¹ for AMBN and ABVN, A are 2.5×10^{16} and 4.1×10^{14} , and the correlation coefficients are 0.991 and 0.993, correspondingly.

Curve-fitting and well-established kinetic equations were based on model-fitting and differential isoconversional methods, respectively. There have been concerns with the accuracy of the curve-fitting approach. From Figs. 2, 3, the faster scanning results in a broader and smoother energy curve, but a more unstable conversion rate of thermal decomposition. Therefore, for the evaluation of AMBN and ABVN thermokinetic parameters of thermal decomposition via non-isothermal kinetics method, an improved result was observed at scanning rates <4 °C min⁻¹, which was determined from the processing of model-fitting or model-free computed AMBN and ABVN's thermokinetic parameters.

Evaluation of thermokinetic parameters via approximate solution

This section considers the development of the mathematical model of the n th-order system under a dynamic experiment.

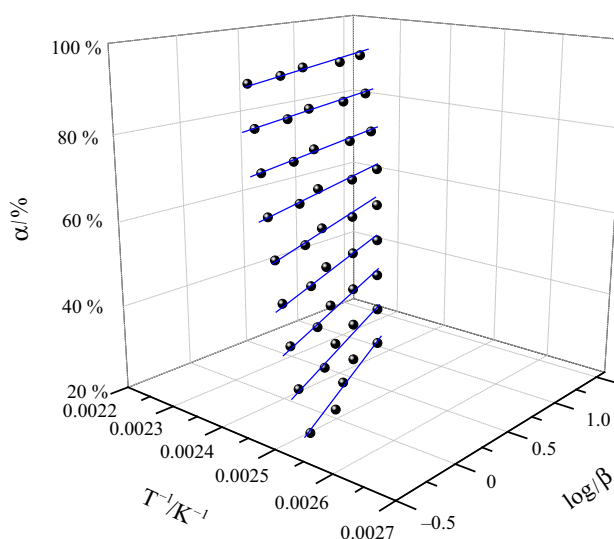


Fig. 5 Activation energy analysis graphs for ABVN at scanning rates of 0.5, 1, 2, 4, and 8 °C min⁻¹ under α at 10, 20, 30, 40, 50, 60, 70, 80, and 90 % by Ozawa–Flynn–Wall kinetic equation

Table 2 Apparent activation energy of AMBN and ABVN determined by Flynn–Wall–Ozawa equation and approximate solution

Equation	Ozawa	Approximate solution	Literature value
AMBN	143	137	141 [6]
ABVN	128	123	133 [1]

Analytical expressions are also derived to be used in the exothermic reaction in the systems with both linear and Frank-Kamenetskii kinetics. The kinetic behaviours of a wide range of an n th-order system can be well approximated through the prototype step:

$$-r_a = -\frac{dC_A}{dT} = k_0 e^{-\frac{E_a}{RT}} C_A^n \quad (2)$$

From the identification of thermal decomposition, the conversion rate is defined as Eq. (3):

$$\alpha = \frac{C_{a0} - C_A}{C_{A0}} \quad (3)$$

Then, integration results in Eq. (4) under the Frank-Kamenetskii approximate solution [22, 23]:

$$\frac{d\alpha}{dT} = \frac{A}{\beta} e^{-\frac{E_a}{RT}} f(\alpha) \quad (4)$$

$$f(\alpha) = (1 - \alpha)^n \quad (5)$$

$$\int_0^\alpha \frac{d\alpha}{f(\alpha)} = \int_{T_0}^T \frac{A}{\beta} e^{-\frac{E_a}{RT}} dT \cong \left(\frac{A}{\beta}\right) \frac{RT^2}{E_a} e^{-\frac{E_a}{RT}} \quad (6)$$

To simplify the complex calculations, we consider $G(\alpha)$ as Eq. (7), then Eq. (9) can be derived from Eqs. (7) and (8) by:

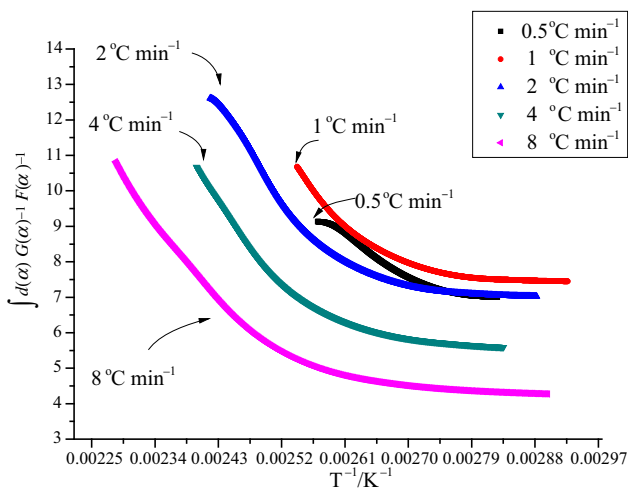


Fig. 6 Calculation for apparent activation energy of AMBN decomposition via approximate solution

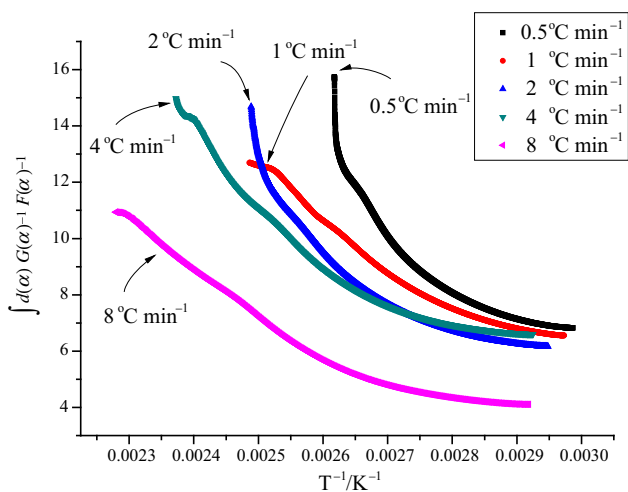


Fig. 7 Calculation for apparent activation energy of ABVN decomposition via approximate solution

$$G(\alpha) = \int_0^\alpha \frac{d\alpha}{f(\alpha)} \tag{7}$$

$$G(\alpha)f(\alpha) = \left(\frac{A}{\beta}\right) \frac{RT^2}{E_a} e^{-\frac{E_a}{RT}} f(\alpha) = \frac{RT^2}{E_a} \frac{d\alpha}{dt} \tag{8}$$

$$\int_0^\alpha \frac{d\alpha}{G(\alpha)f(\alpha)} = \int_0^T \frac{E_a}{RT^2} dT = -\frac{E_a}{R} \frac{1}{T} + \text{const} \tag{9}$$

Therefore, the E_a value of AMBN and ABVN under the n th-order reaction assumption can be estimated using Eq. (9) with Frank-Kamenetskii approximate solutions. Figures 6, 7 show the regions of exothermic characteristics of the patterns generated in the reaction process that can be exactly determined mathematically. Finally, the E_a values calculated via the approximate solution are 137 and

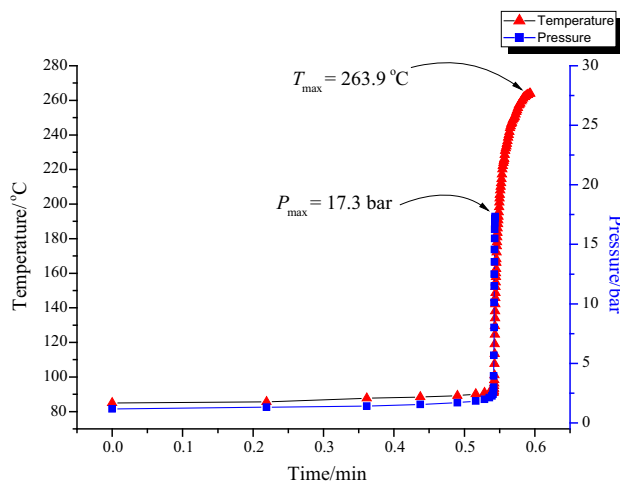


Fig. 8 Temperature and pressure versus time curves for AMBN by VSP2 test

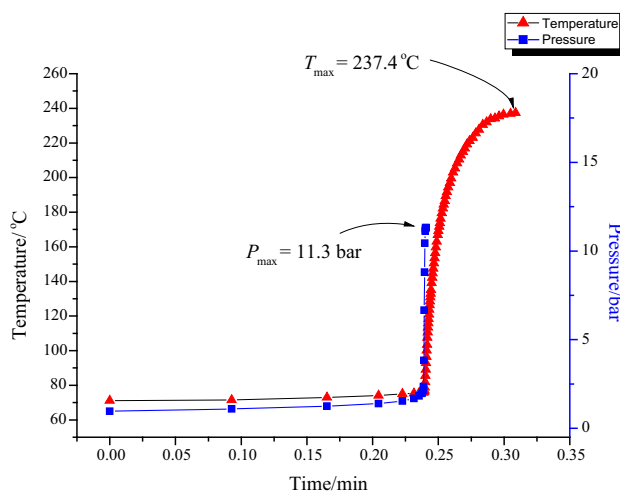


Fig. 9 Temperature and pressure versus time curves for ABVN by VSP2 test

123 kJ mol⁻¹, A are 3.1×10^{18} and 5.1×10^{16} , and the correlation coefficients are 0.987 and 0.982 for AMBN and ABVN, respectively, as listed in Table 2. This method identifies the additional parameters needed to estimate the E_a value applied in the reactant self-accelerating decomposition temperature ($SADT$), which can identify the lowest external temperature at which the reactive chemical might produce any exothermic decomposition reactions when it is stored in the tank or in the delivery process [24].

Comparison of the thermal hazard with DSC and VSP2 tests

Studies have shown that at 98 mass%, the AMBN and ABVN exothermic phenomena occur when the reaction is

Fig. 11 Heat flow (a), self-heating rate (b), and pressure rise rate (c) versus temperature of ABVN by DSC and VSP2 tests

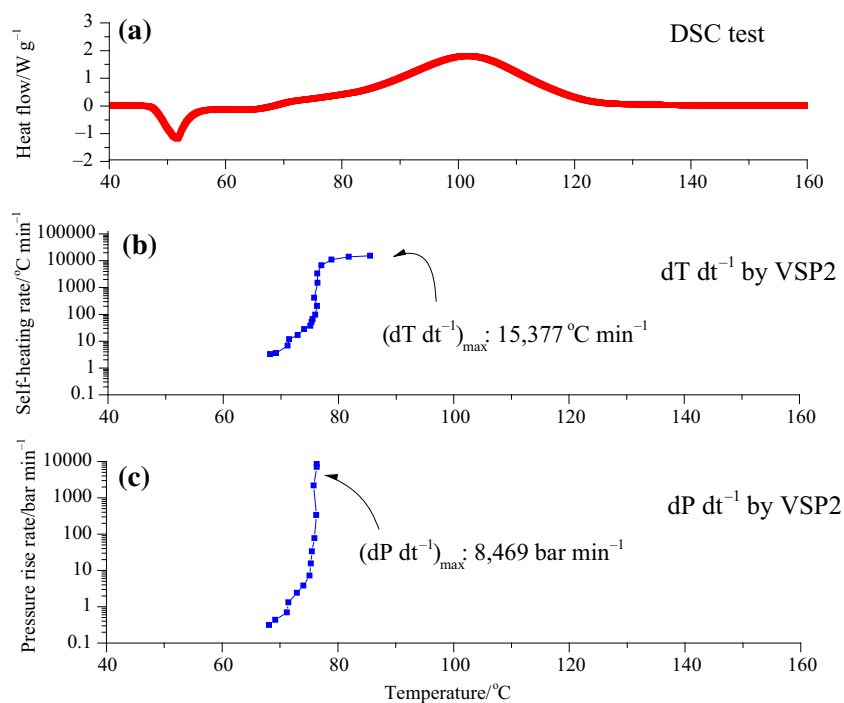
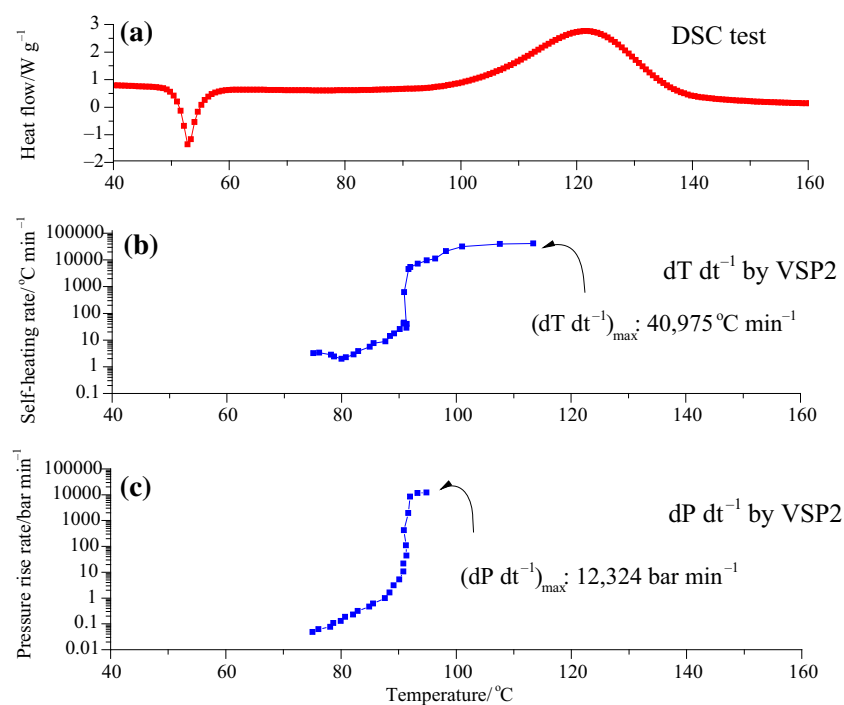


Fig. 10 Heat flow (a), self-heating rate (b), and pressure rise rate (c) versus temperature of AMBN by DSC and VSP2 tests



at 78 and 66 $^{\circ}\text{C}$, respectively. Because the temperature constantly and cumulatively increases, 5 g of the samples can result in a reaction temperature up to 264 and 237 $^{\circ}\text{C}$

under adiabatic conditions for AMBN and ABVN, respectively, and a reaction pressure up to 11.3 and 17.3 bar. During runaway reactions, the temperature increases at a

Table 3 Adiabatic parameters of runaway characteristics for AMBN and ABVN by VSP2

Reactant		$T_0/^\circ\text{C}$	$T_{\text{max}}/^\circ\text{C}$	$P_{\text{max}}/\text{bar}$	$(dT dt^{-1})_{\text{max}}/^\circ\text{C min}^{-1}$	$(dP dt^{-1})_{\text{max}}/\text{bar min}^{-1}$
Material	Mass/g					
98 mass% AMBN	5 ± 0.5	78	264	17.3	40,975	12,324
98 mass% ABVN		66	237	11.3	15,377	8,469

rate of 40,975 and 15,377 $^\circ\text{C min}^{-1}$ for AMBN and ABVN, respectively, and the pressure increases at a rate of 12,324 and 8469 bar min^{-1} , as shown in Figs. 8, 9, 10, 11. Table 3 lists reliable parameters for industrial processes.

The thermal curve results were combined by DSC and VSP2, as shown in Figs. 10, 11. In accordance with DSC tests, the T_0 followed the reaction characteristics and rudimentary thermal hazards when azo compound was decomposed under non-isothermal conditions. From the VSP2 tests, this study could validate the correspondence of DSC results by $(dT/dt)_{\text{max}}$ and $(dP/dt)_{\text{max}}$ under adiabatic conditions. The exothermic behaviours of solid azo compounds, such as AMBN and ABVN, was obvious in that the self-heating and pressure rise rate increased for <1 s from onset to apex. The potential hazard of reaction is subject to dT/dt and dP/dt by adiabatic conditions. Moreover, the thermal hazard could be determined whether the runaway reaction occurred for the assessment of loss prevention concerns, alleviating the frequency of potential disasters [25–30].

The T_0 , $dT dt^{-1}$, and $dP dt^{-1}$ of AMBN and ABVN were confirmed at the same time for understanding the hazardous characteristics by synergizing DSC and VSP2 test data. The temperatures during the beginning of the decomposition of AMBN and ABVN were approximately 80 and 70 $^\circ\text{C}$, respectively. The runaway behaviours of DSC and VSP2 matched approximately. In general, the timing of temperature by VSP2 was slightly slower than DSC, which was unavoidable. The difference between VSP2 and DSC is that the DSC test cell was offered energy five heating source continuously, even when the self-heating reaction occurred at the same time.

Conclusions

The effect of the runaway reaction for AMBN and ABVN was evaluated using DSC and VSP2 by dynamic and adiabatic methods, according to the thermal decomposition from various thermokinetic parameters as well as thermal curves and the E_a values acquired from the Flynn–Wall–Ozawa equation and approximate solution. In an actual manufacturing process, in addition to the high reactivity of AMBN and ABVN, the initiator content may become a key substance, resulting in runaway excursions.

Acknowledgements The authors appreciate the financial supports from the Ministry of Science and Technology (MOST) of the ROC under Grant Nos. NSC 98-2221-E-407-002-MY3 and NSC 101-2221-E-407-0001-MY3.

References

1. Van Hook JP, Tobolsky AV. The thermal decomposition of 2,2'-azo-bis-isobutyronitrile. *J Am Chem Soc.* 1975;80:779–82.
2. Liu SH, Yu YP, Lin YC, Weng SY, Hsieh TF, Hou HY. Complex thermal evaluation for 2,2'-azobis(isobutyronitrile) by non-isothermal and isothermal kinetic analysis methods. *J Therm Anal Calorim.* 2014;116:1361–7.
3. Harfi JE, Kingman SW, Dimitrakis G, Robinson JP, Irvine DJ. Dielectric properties of free radical initiators-Investigation of thermal decomposition products. *Ind Eng Chem Res.* 2012;51:15811–20.
4. Smith AD, Lester EH, Thurecht KJ, Kingman SW, Harfi JE, Dimitrakis G, Robinson JP, Irvine DJ. Temperature dependence of the dielectric properties of 2,2'-azobis(2-methyl-butyronitrile) (AMBN). *Ind Eng Chem Res.* 2010;49:3011–9.
5. Li XR, Wang XL, Koseki H. Study on thermal decomposition characteristics of AIBN. *J Hazard Mater.* 2008;159:13–8.
6. Li XR, Koseki H. SADT prediction of autocatalytic material using isothermal calorimetry analysis. *Thermochim Acta.* 2005;431:113–6.
7. Li XR, Koseki H. Study on the early stage of runaway reaction using Dewar vessels. *J Loss Prev Process Ind.* 2005;18:460–4.
8. Ho SK. The thermal decomposition of azo-compounds in solution. Pokfulam: The University of Hong Kong; 1960.
9. Gowda S, Abiraj K, Gowda DC. Reductive cleavage of azo compounds catalyzed by commercial zinc dust using ammonium formate or formic acid. *Tetrahedron Lett.* 2002;43:1329–31.
10. Sun CK, Zhao HM, Fang DC, Li ZH. Theoretical study on the thermal decomposition of azoisobutyronitrile. *J Mol Struct.* 2004;679:89–94.
11. Dubikhin VV, Knerel'man EI, Manelis GB, Nazin GM, Prokudin VG, Stashina GA, Chukanov NV, Shastin AV. Thermal decomposition of azobis(isobutyronitrile) in the solid state. *Kinet Catal.* 2012;446:171–5.
12. Partington S, Waldram SP. Runaway reaction during production of an azo dye intermediate. *Process Saf Environ Prot.* 2002;80:33–9.
13. Talat E, Bywate S. The thermal decomposition of 2,2'-azo-bis-isobutyronitrile. *J Am Chem Soc.* 1954;77:3712–4.
14. Steensma M, Schuurman P, Malow M, Krause U, Wehrstedt KD. Evaluation of the validity of the UN SADT H.4 test for solid organic peroxides and self-reactive substances. *J Hazard Mater.* 2005;A117:89–102.
15. STARe Software with Solaris Operating System. Operating instructions. Switzerland: Mettler Toledo; 2015.
16. Liu SH, Lin CP, Shu CM. Thermokinetic parameters and thermal hazard evaluation for three organic peroxides by DSC and TAM III. *J Therm Anal Calorim.* 2011;106:165–72.

17. Chu YC, Chen JR, Tseng JM, Tsai LC, Shu CM. Evaluation of runaway thermal reactions of di-tert-butyl peroxide employing calorimetric approaches. *J Therm Anal Calorim.* 2011;106:227–34.
18. Townsend DI, Tou JC. Thermal hazard evaluation by an accelerating rate calorimeter. *Thermochim Acta.* 1980;37:1–30.
19. Flynn JH, Wall LA. A quick, direct method for the determination of activation energy from thermogravimetric data. *J Polym Sci Part B Polym Lett.* 1966;4:323–8.
20. Ozawa T. A new method of analyzing thermogravimetric data. *Bull Chem Soc.* 1965;38:1881–6.
21. Doyle CD. Series approximations to the equation of thermogravimetric data. *Nature.* 1965;207:290–1.
22. Frank-Kamenetskii DA. Diffusion and heat exchange in chemical kinetics. New Jersey: Princeton University; 1955.
23. Frank-Kamenetskii DA. Diffusion and heat exchange in chemical kinetics. 2nd ed. New York: Plenum Press; 1969.
24. Liu SH, Shu CM, Hou HY. Applications of thermal hazard analyses on process safety assessments. *J Loss Prev Process Ind.* 2015;33:59–69.
25. Tseng JM, Liu MY, Chen SL, Hwang WT, Gupta JP, Shu CM. Runaway effects of nitric acid on methyl ethyl ketone peroxide by TAM III test. *J Therm Anal Calorim.* 2009;96:789–93.
26. Tseng JM, Shu CM. Isothermal kinetic evaluation of methyl ethyl ketone peroxide mixed with acetone by TAM III tests. *Thermochim Acta.* 2010;507–8:45–8.
27. Tsai YT, You ML, Qian XM, Shu CM. Calorimetric techniques combined with various thermokinetic models to evaluate incompatible hazard of tert-butyl peroxy-2-ethyl hexanoate mixed with metal ions. *Ind Eng Chem Res.* 2013;52:8206–15.
28. Brauner N, Shacham M. Statistical analysis of linear and non-linear correlation of the Arrhenius equation constants. *Chem Eng Prog.* 1997;36:243–9.
29. Torfs JCM, Deij L, Dorrepaal AJ, Heijens JC. Determination of Arrhenius kinetic constants by differential scanning calorimetry. *Anal Chem.* 1984;56:2863–7.
30. Vyazovkin S. Mechanism and kinetics of epoxy-amine cure studied by differential scanning calorimetry. *Macromolecules.* 1996;29:1867–73.